STATUS OF THE TARN II PROJECT

T. Tanabe
Institute for Nuclear Study, University of Tokyo,
Tanashi, Tokyo 188, Japan

Summary

The construction of a synchrotron-cooler ring TARN II is currently in progress. Maximum energies of this machine are 1 GeV for proton and 340 MeV/u for heavy ions with charge to mass ratio of q/A=1/2. After acceleration, the beams with energies up to 200 MeV/u can be cooled by an electron cooling device in the ring. Present status of the construction is described.

Introduction

At the Institute for Nuclear Study, University of Tokyo, a small storage ring for low energy ion beam, TARN, had been used since 1979 for the studies of accelerator technology such as beam stacking in both transverse and longitudinal phase spaces and stochastic momentum cooling of ion beams[1]. This machine was shut down in 1985 in order to construct a newly extended machine, since dc characteristics of the dipole magnets and rather short length of the straight sections limited studies such as a synchrotron acceleration, an electron cooling and a beam ejection.

The new accelerator TARN II which takes the place of the old one is designed to accelerate ion beams as well as storage. Another new feature of this machine is that the phase space density of the stored ion beams is compressed by using an electron cooling device. The electron cooling can be considered as a promising technique complementing the stochastic cooling. The primary aim of the machine is in the development of the accelerator technology which can be applied to the design of future machines. On the other hand, the electron cooling process itself is an interesting subject for physics and also the cooled good quality beams can serve as excellent probes for atomic and nuclear physics studies. Such application of this ring is also expected in future.

In the following, the outline of the ring and the electron cooling device is presented. Description of a candidate of internal targets is also given.

The Ring

Layout of the ring is shown in Fig. 1. The ring is regular hexagonal in shape with the average diameter of 24 m. The circumference is determined to be 17 times of that of the outermost orbit of the injector cyclotron so as to allow synchronous beam transfer between both accelerators. Six long straight sections are used for the injection, the slow extraction, the rf equipment, the electron cooling, the stochastic cooling and the internal target station. The diameter of the ring was limited by the size of the existing building. Beams are injected into one of the six long straight sections from an existing sector focusing cyclotron. The main parameters of the ring are listed in Table 1. The

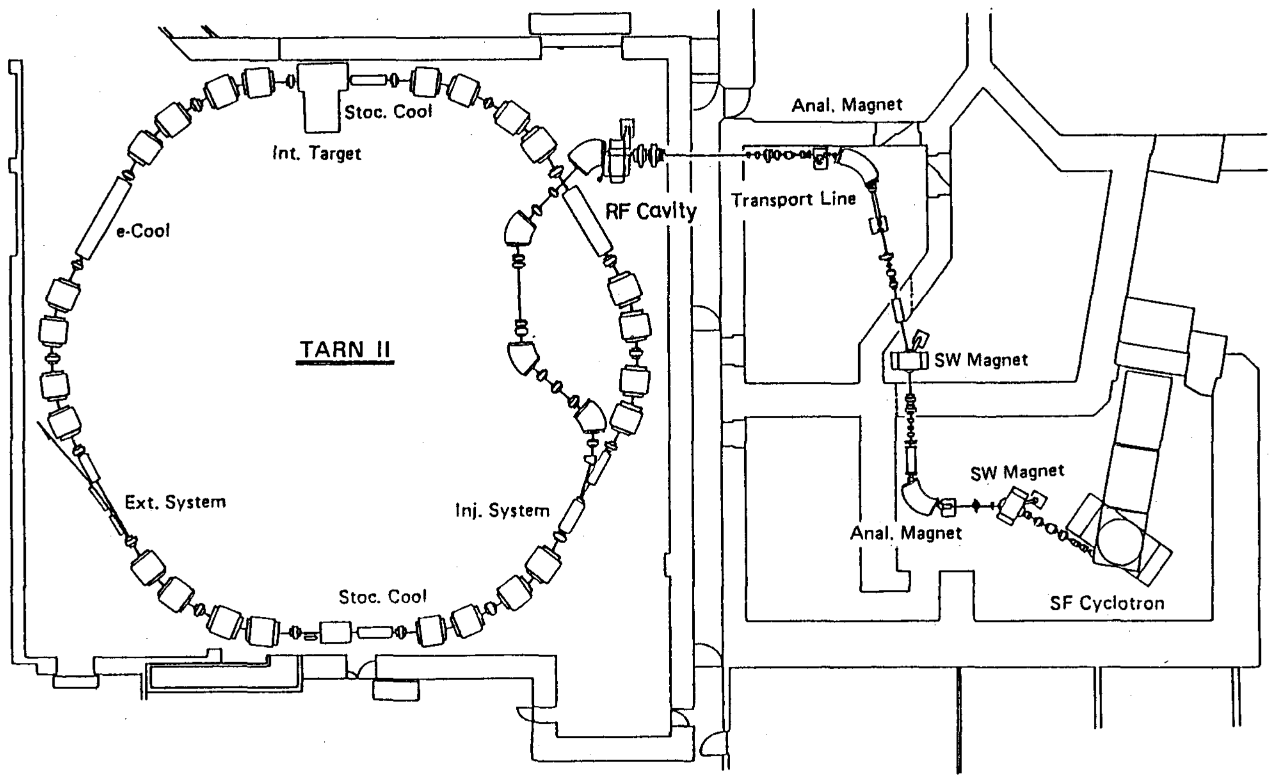

Fig. 1. Layout of TARN II and injector SF cyclotron.

Table 1. TARN II Parameters

Maximum $B\rho$	5.8 Tm (6.8)
Maximum beam energy proton	1 GeV (1.3)
ions with q/A=1/2	340 MeV/u (450)
Circumference	77.76 m
Average radius	12.38 m
Radius of curvature	3.82 m
Focusing structure	FBDBFO
Length of long straight section	4.2 m
Superperiodicity for mode I	6
" mode II	3
Betatron tune value ν_x/ν_y for mode I	1.75/1.25
" mode II	1.75/1.25
Transition γ for mode I	1.85
" mode II	2.97
Rising time of magnet excitation	3.5 sec (0.75)
Repetition rate	0.1 Hz (0.5)
Maximum field of dipole magnets	15.2 kG (18)
Maximum gradient of quadrupole magnets	70 kG/m
Revolution frequency	0.31-3.75 MHz
Acceleration frequency	0.61-8 MHz
Harmonic number	2
Maximum rf voltage	6 kV
Useful aperture	50×200 mm^2
Vacuum pressure	10^{-11} Torr

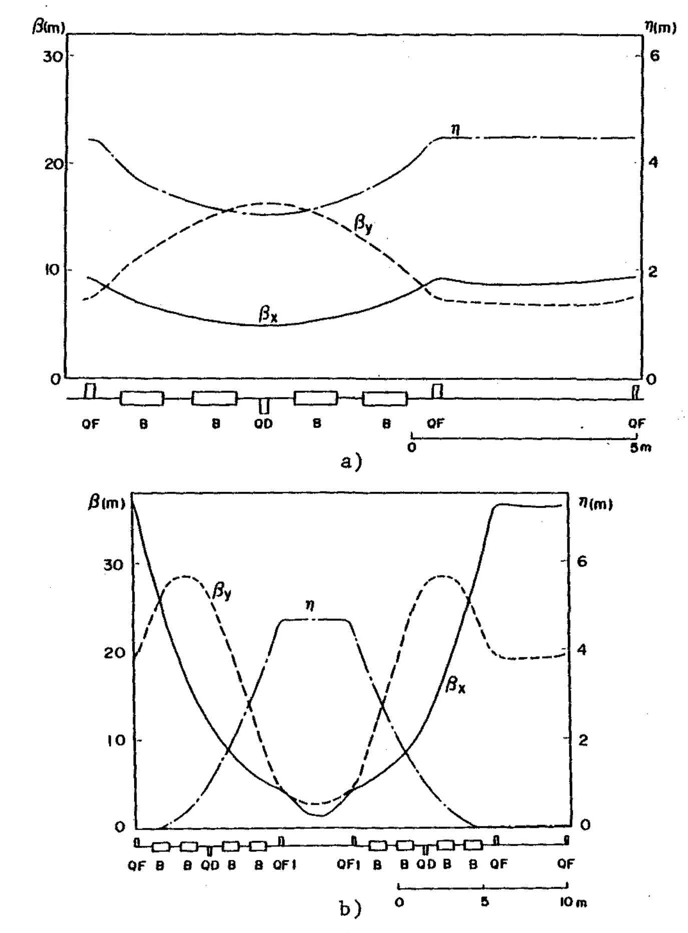

Fig. 2. Beta and dispersion functions of the TARN II. a) Mode I (Synchrotron mode), b)Mode II (Cooler-ring mode). Tune values for both modes are 1.75 and 1.25 in horizontal and vertical directions, respectively.

maximum magnetic rigidity of the dipole magnet is designed as 6.8 Tm. However, the maximum magnetic field and the rising time of the dipole magnets are limited by the capacity of the electric power substation available at the present moment. So we begin with the maximum magnetic rigidity of 5.8 Tm and the values in the parentheses in the table will be realized in the second phase of the project.

Lattice and operation mode

Lattice consists of 24 dipole and 18 quadrupole singlet magnets[2]. We have two modes of operations depending on different purposes. The mode I corresponds to the usual synchrotron operation, in which beams are accelerated and then extracted in 0.1 Hz. On the other hand, for the mode II beams are cooled at the long flat top of the magnet excitation after acceleration. The former and the latter correspond to the external and the internal target experimental use, respectively. The focusing structure is based on a simple FODO lattice because of its compactness so as to realize the higher maximum energy within the limited space. Long straight sections of 4.2 m in length are inserted between horizontally focusing quadrupole magnets at every unit cell. The whole circumference is composed of six unit cells. For the mode I, these cells are all excited identically. The acceptance as large as 400π mm·mrad is realized by small maximum β-values as shown in Fig. 2. For the mode II, the dispersion function in the cooling section has to be minimized to keep a large stable region and furthermore the amplitude function in the internal target section should be small. So as to realize these demands, the superperiodicity of the lattice for the mode II is reduced to three with changes of only excitation patterns of quadrupole magnets. Rather large β-functions in the cooling section as shown in Fig. 2 reduce the radial acceptance of this mode to 70π mm·mrad.

Magnets

Quadrupole magnets of 20 cm in length are made of laminated core of 0.5 mm in thickness. The pole shape with a bore radius of 65 mm is hyperbola smoothly connected to its tangential lines at both sides.

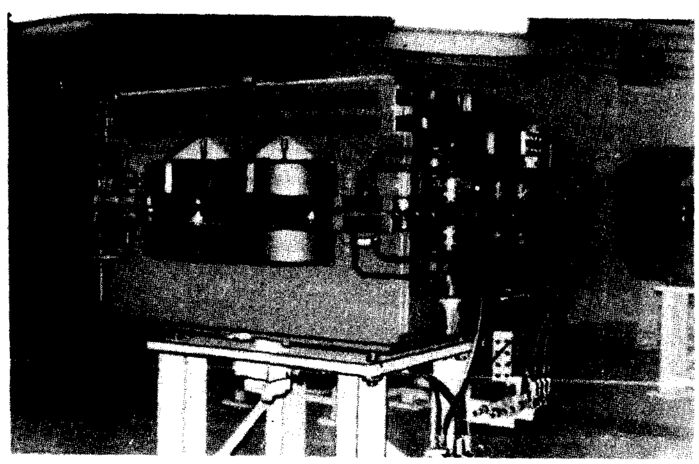

Fig. 3. A dipole magnet for the TARN II. Backleg coils are also wound around the magnet yokes, which produce a bump field for the beam extraction.

28 Заказ № 780

For the dipole magnet, H-type is adopted, because its field uniformity is better than the one of the C-type and also its coils are located at lower magnetic field position and shielded from high radiation region in comparison with those of the window-frame type. The magnet is straight in shape because of the easiness of fabrication and its length is rather short (1 m) to reduce the saggita to a reasonable value (16.4 mm). The magnet core is made of laminated silicon steel strip of 0.5 mm in thickness. The useful aperture and width are 8 cm and 20 cm, respectively. The pole edges are shaped with B-constant curve and also small shims connected smoothly to the curve are attached in order to realize the uniform field for the wide range of excitation levels up to 18 kG. All of the magnet system of the ring have already been constructed. Figure 3 shows a photograph of one of the dipole magnets. The magnetic field was measured in detail and its typical example is shown in Fig. 4. There are field bumps in both sides at low excitation levels and they disappear at the high field. A good field region of ± 10 cm is attained as seen in the figure.

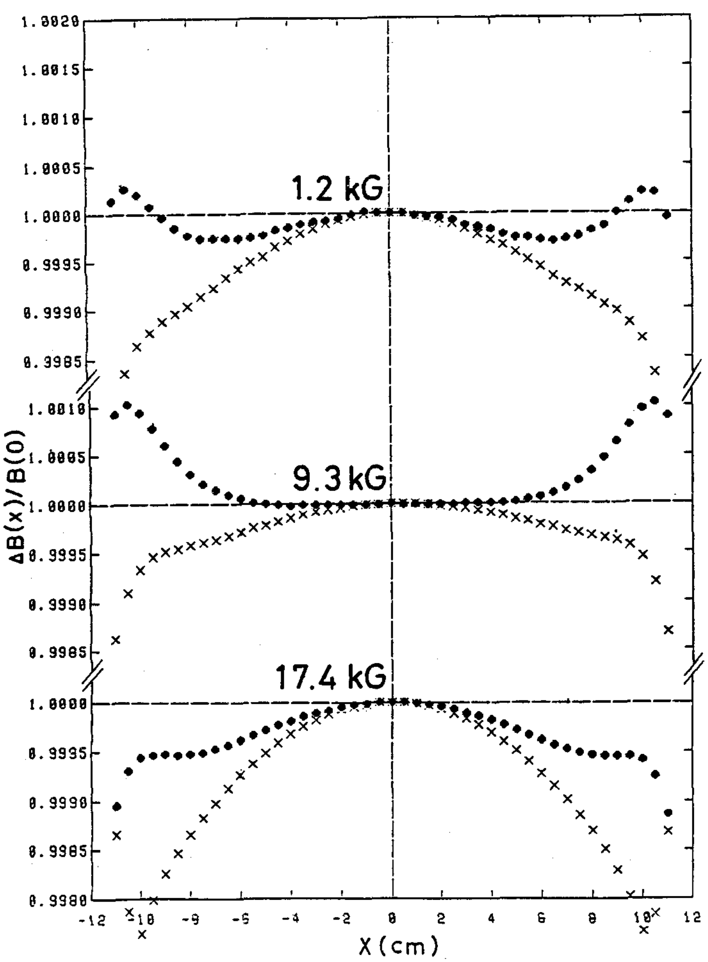

Fig. 4. Radial field distribution of the dipole magnet for different excitation levels. Points show the field at the center of the magnet. Crosses represent the field distribution integrated along the beam path.

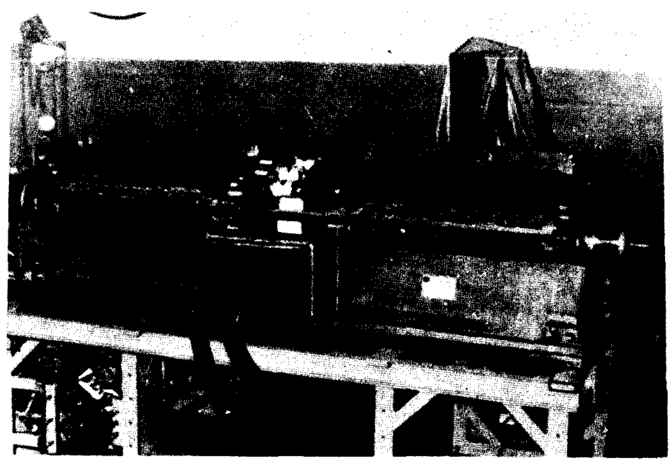

Fig. 5. The rf cavity.

Rf Acceleration System

The system is operated from 0.61 MHz to 8 MHz in harmonic number of 2 with maximum rf voltage of 6 kV. The voltage was determined on the assumption of the repetition frequency of 0.5 Hz in the final goal of our project. The lowest frequency of 0.61 MHz corresponds to the injection energy of 3 MeV/u. The adiabatic capture and acceleration require the frequency range of 0.61–7.02 MHz, while the synchronous beam transfer between the SF cyclotron and the TARN II requires the range of 7.32–8 MHz. In this way the sweeping range of the rf frequencies is very wide due to the low injection energy. This requires the development of an rf cavity loaded with high initial permeability ferrites. A ferrite commercially available, TDK SY-6, was chosen because it can cover the required wide range in tunable frequencies. A single-gap rf cavity of two ferrite-loaded $\lambda/4$ coaxial resonators has been constructed[3]. The picture of the rf cavity is shown in Fig. 5. In a half of the cavity, 24 ferrite rings are stacked alternately with water-cooled copper plates. The total length of the cavity is 2.55 m. For the ferrite-bias current, supplementary windings are also wound together with the main ones in a symmetric "figure of eight" configuration. The supplementary ones are excited by a constant dc current in opposite direction to the main current. A sum of these two currents can be assumed as a net current. Thus a net "zero" current is achievable with good current stability. Tuning frequencies have successfully been varied by a factor of 13.2 in a change of the net ferrite bias current from 0 to 750 A. It has been found from low-level rf measurements on rf characteristics that most of the design goals have been attained. Ultra-high vacuum of a beam tube has been achieved with a pressure of 1×10^{-10} Torr after heating the inner conductors up to 350°C. The other parts of the whole rf system are under design.

Injection

Beams are injected from the sector focusing cyclotron[4] with K-number of 68. Energies and intensities of typical beams from proton to neon extracted from the cyclotron are listed in Table 2. Naked heavy ion beams are injected into the ring after fully stripped by a thin foil. For the stripper, we have succeeded in the developments of excellently long-lived carbon foils[5]. The beam intensity in the ring for each operation mode is estimated assuming the multi-turn injection and the

Table 2. Typical ion beams from SF cyclotron

	H^+	$^6Li^{2+}$	$^{11}B^{3+}$	$^{12}C^{4+}$	$^{14}N^{4+}$	$^{16}O^{5+}$	$^{20}Ne^{6+}$
T(MeV/u)	20	7.6	5.1	7.6	5.5	6.6	5.8
I(eμA)	100	14	9	15	17	5	12

transport efficiency at each point. For the mode I, the number of ions injected into the ring is about 10^9 for light ions and about 10^7 for heavy ions. For the mode II, on the other hand, the numbers are less than those of the mode I by a factor of 6, due to the limited acceptance.

The space charge limit on the stored beam intensity is much higher than the stacked intensity by the multi-turn method. As the beam intensity is not high enough especially for the mode II, some possibilities to increase the intensities have been discussed:

1) Beams are multi-turn injected into the acceptance of 400π mm·mrad of the mode I which is larger than the one of the mode II. After pre-cooling in the transverse direction by the stochastic cooling method in around 20 seconds, the beam is accelerated with the mode I up to the desired energy. Then the mode is smoothly changed from the mode I to the mode II, keeping the operation point at the same values of ($\nu_H \sim 1.75$, $\nu_V \sim 1.25$) by changing the excitation levels of the lattice quadrupole magnets. In this method the intensity increase by a factor of 6 is expected[2].

2) The second one is so-called stripping-injection method. In this case, H_2^+ beams of 34 MeV in energy are injected and changed to H^+ ion beams through a thin foil inserted in the ring. If we assume maximum allowable emittance growth of 10π mm·mrad and momentum spread $\Delta p/p=\pm 0.2\%$, a stacking factor of about 160 turns should be achievable, which corresponds to the intensity increase approximately by two orders of magnitude in comparison with the one of the multi-turn injection method. However, this method is not applicable to heavier ions since the injection energies are not high enough and so the number of passage of ions through the foil is extremely limited due to the large emittance growth and the energy loss in the foil. In addition to this, the probability of fully stripping decreases with the atomic number and this also limits the number of the injection for heavier ions.

3) It is intended to increase the intensity by injecting beams from a linac system with energy of about 3 MeV/u in future. In this case, the intensity is expected to increase by two orders of magnitude. The first stage of the linac system, an RFQ linac has already been constructed and tested[6]. This can accelerate ions with $\varepsilon = q/A = 1 \sim 1/7$ from 8 keV/u up to 800 keV/u. The operating frequency is 100 MHz. The cavity is 58 cm in diameter and 730 cm in length. The designed beam intensity is $1/\varepsilon$ mA. Figure 6 shows the photograph of this linac called TALL. The beam test was carried out by using proton beam and a transmission exceeding 90 % was obtained at the current of 10 μA. The energy spread of the output beam was 1.6 % in FWHM.

Extraction

A slow extraction channel is being planned to meet demands for experiments. Beams are spilt by using third-integer resonance ($\nu_H \sim 5/3$) at the flat-top of the magnet excitation[7]. A part of circulating particles is driven into the resonance and becomes unstable by the perturbation of sextupole magnets. The extraction system consists of an electrostatic septum, three septum magnets, and four bumps which are produced by backleg coils wound on the main dipole magnets. The electrostatic septum which is the first channel for the extraction system has been completed as shown in Fig. 7. In order to increase the extraction efficiency, the septum is made of the W-Re wires as thin as 90 μm in diameter with a spacing of 1.25 mm. The length of the septum is 1 m and the maximum electric field is 60 kV/cm for a gap of 2 cm. The horizontal deflection is 4 mrad at the maximum field for 1 GeV proton.

Electron Cooling

The electron cooling device[8,9] can cool ion beams with energy up to 200 MeV/u in the ring. The main parameters of the cooling system are listed in Table 3. The length of the interaction region of 1.5 m is limited by the rather short length of the straight section of the ring. The diameter of the electron

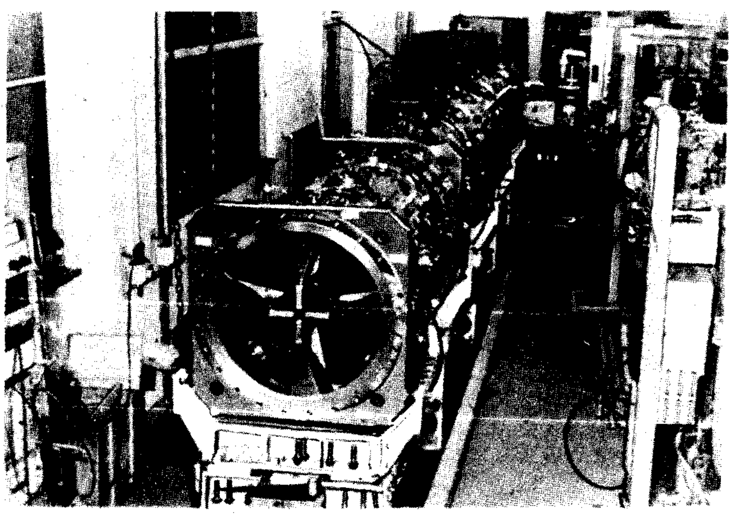

Fig. 6. View of the RFQ linac "TALL".

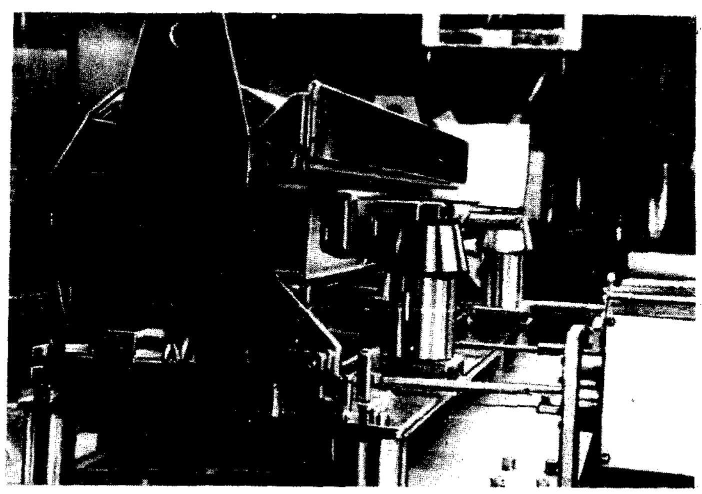

Fig. 7. Electrostatic septum for the slow extraction system.

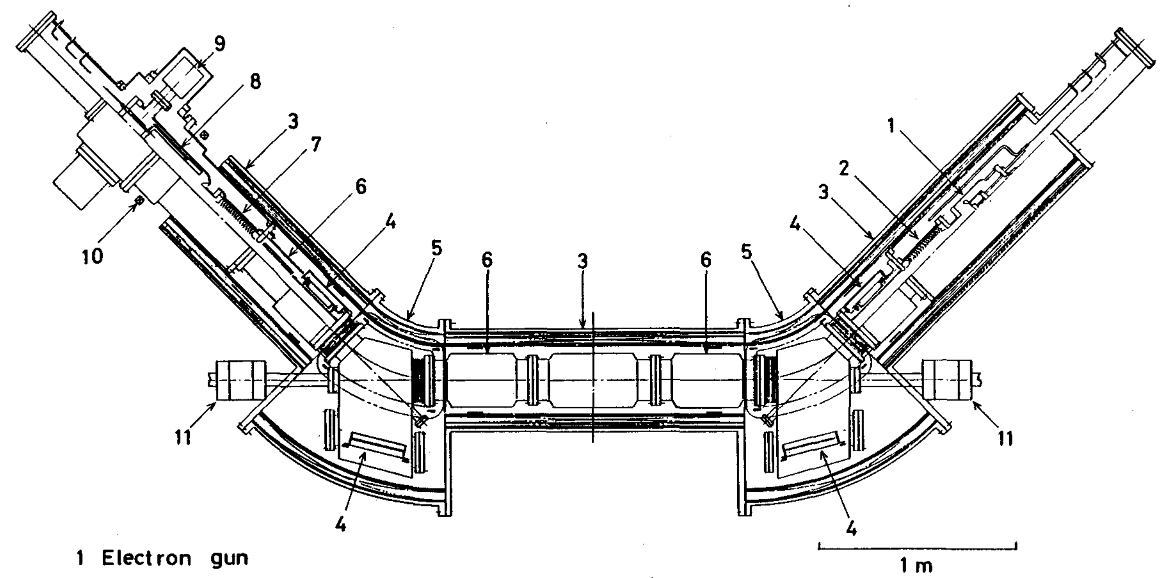

Fig. 8. Layout of electron cooling device.

Table 3. Electron cooling parameters

Maximum working energy	ion 200 MeV/u electron 120 keV
Cooled ions	H^+ - $^{20}Ne^{10+}$
Length of interaction region	1.5 m
Maximum electron current density	0.5 A/cm^2
Cathode diameter	50 mm
Maximum electron current	10 A
Maximum solenoid field	1.2 kG

beam is 50 mm, which is large enough to cover the ion beam diameter. The layout of the cooling device is shown in Fig. 8. The shape is so-called U-scheme, in which electrons are injected and ejected over the beam line of the ring.

In order to minimize transverse electric field components, the flat cathode is surrounded by the Pierce electrode. The electron gun system and the acceleration column are immersed in a uniform magnetic field so as to guide the electrons and restrict transverse motion to an acceptable amount. Figure 9 shows the electron trajectories in the gun region, which are calculated with the help of SLAC program[10]. The internal electrodes of the accelerating tube have crooked shape in order to protect the ceramic surface from the ions and electrons emanating from the anode and cathode and

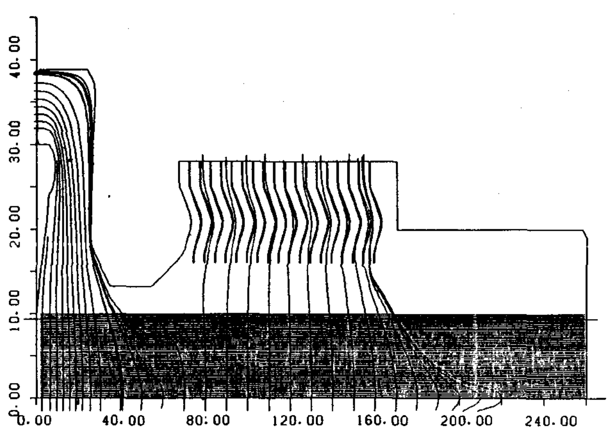

Fig. 9. Calculated electron trajectories in gun. The electron energy and the current are 110 keV and 10 A, respectively. The solenoid field is 1.06 kG.

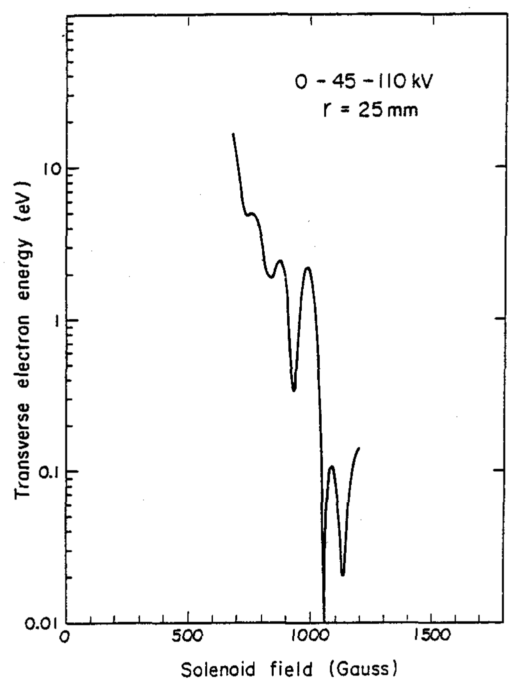

Fig. 10. Transverse energy of outermost electrons as a function of solenoid field.

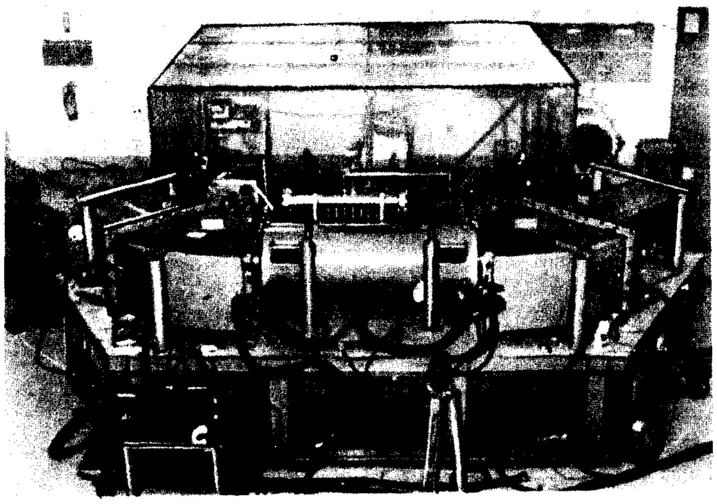

Fig. 11. Electron guiding coils.

also to shield the electron beam from the electrostatic effect of the charges deposited on the ceramic walls. The transverse electron temperature depends greatly on the solenoid field as well as the shape and the geometry of the electrodes. The outermost electrons have generally its highest values. Figure 10 shows the relation of the transverse temperature of these electrons vs. magnetic field. In this calculation, we set the anode voltage at 45 kV which produces electron current of 10 A and the final electron energy was chosen to be 110 kV. As seen in the figure, the temperature less than 0.1 eV is attained at the field below 1.2 kG. Thus the maximum solenoid field is determined to be 1.2 kG.

The most important function of the collector is to gather the electrons with high efficiency because the lost electrons become the load of a highly stabilized high voltage power supply. We adopt the type similar to the Fermilab collector which is a kind of triode, because of its excellent collection efficiencies[11].

The magnet system consists of three solenoids with inner diameter of 36 cm and two 45°-toroids. The diameter of the solenoid is a minimum size to ensure the stable high voltage holding capability at 120 kV in the gun and collector regions. Figure 11 shows a photograph of the magnet system. In order to realize the uniform field along the electron path, several supplementary coils for field corrections are installed at the electron gun region and at each transition region between solenoid and toroid. The gradually vanishing field at the collector region where the electron beam diverges is formed by a pair of correction coils. In the toroids, dipole fields are added in order to cancel the drift of electron due to the centrifugal force. There are also alignment dipole coils for each solenoid to allow for the steering of the electron beam. The whole coils are covered by iron shieldings 15 mm thick except the windows needed for the passage of the electron and ion beams. The three components of the magnetic field were measured with high precision by using three Hall probes (Siemens SBV 601) which were automatically positioned with a driving mechanism composed of ball screws and pulse motors in the three dimensional coordinate space. The results of the field measurements are shown in Fig. 12, which demonstrate the high quality of the magnetic field already achieved.

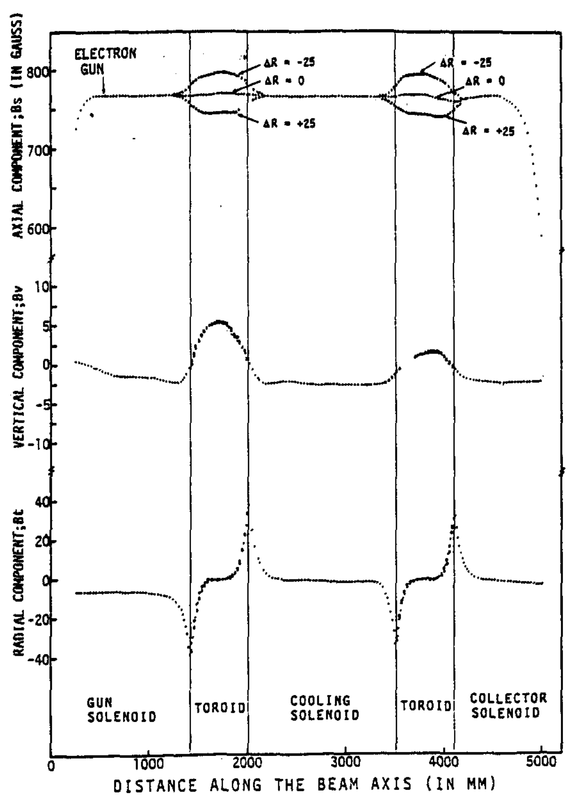

Fig. 12. Magnetic field components for the electron guiding coils along the electron beam.

The high voltage system for the cooling device consists of a 120 kV-20 mA high voltage power supply (HVPS) for the acceleration and deceleration of electrons, a gun anode PS (50 kV-20 mA), a collector PS (6 kV-10 A) and a collector anode PS (6 kV-20 mA). All of them except the HVPS are housed in a high voltage platform with the maximum voltage of 120 kV. The longitudinal electron temperature is mainly determined by the stability of the HVPS. The stability of $\pm 1\times10^{-5}$ has already been achieved at 120 kV. The electron space charge gives rise to an unwanted tune shift in the ion orbits especially at the low energy during injection and acceleration. In order to suppress the electron current during such periods, the gun anode PS which determines the electron current is designed to allow fast switching (1 msec) of the electron beam synchronized with the cycling of the TARN II. It is driven by a series tube with fast rising time.

Vacuum is attained by using four groups of non-evaporable getter (NEG) pumps (Saes ST707) installed close to the cathode and the collector and also inside both toroid chambers. These provide total pumping speed of 8000 l/s for H_2 at room temperature. Drift tubes, electrostatic position monitor electrodes and antennas to pick up microwave emitted by the spiral motions of the electrons in the magnetic field are set inside the vacuum chamber.

The time evolution of the beam emittance and momentum spread for the combined system of the cooling device and the storage ring is complicated process and cannot be predicted with a simple mathematical expression. The cooling process as a function of time was studied with help of the simulation program SPEC[12] developed by the KfK group at CERN. A typical example is shown in

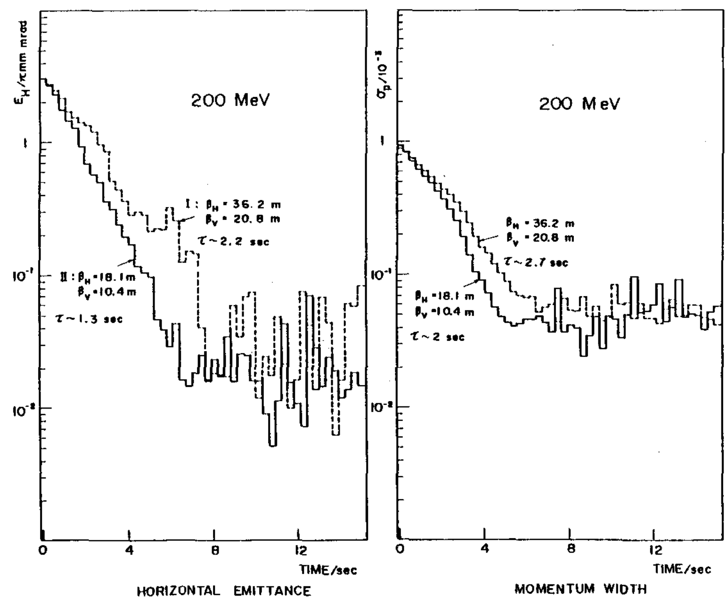

Fig. 13. Time evolution of emittance and momentum width of cooled ions after injection. Those for different amplitude functions are compared.

Fig. 13. We can expect the cooling time of a few seconds for our cooling system. The cooling rate varies significantly with changes of the lattice parameters of the ring as well as the cooling device itself[13]. When an internal target is inserted into another straight section, the equilibrium beam energy spread is proportional to the products of the target thickness and the beta functions at the target and at the cooling section[14]. In this connection, studies for optimization of lattice parameters have to be continued also taking account of the beam heating due to the insertion of the internal target.

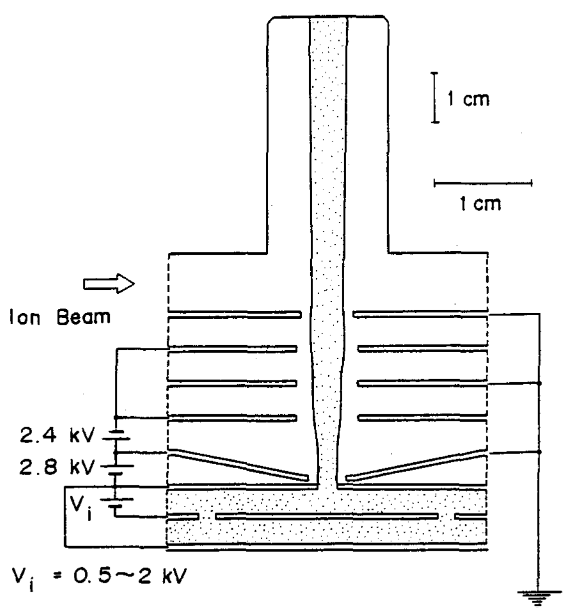

Fig. 14. Microparticle internal target.

Internal Target

The use of the cooler ring with an internal target is very attractive for the nuclear physics experiments. We have started studying the internal target for the research of physics in future. There are lots of candidates for the internal targets[15]. Among these a microparticle target has been adopted for a feasibility study, because microparticles are commercially available for most solid materials and the apparatus can be made inexpensively in comparison with the gas jet target which has already been established. Figure 14 shows a layout of this target. Microparticles are negatively contact-charged between the lower parallel plates. The negative charge is preferable for the internal target, since positively charged particles are repelled by the ion beam space charge at the interaction region[15]. Charged particles emerging through a hole with a diameter of 1 mm are accelerated and then collimated by einzel lenses. Ion beams intersect perpendicularly with the microparticle flux at the exit from the lenses. The target thickness was estimated by measuring events of elastically scattered ions. In a test, nickel microparticles of 1 μm in average diameter are accelerated at about 4 kV. The size of this particle flux at the interaction region with ions is around 4 mm in diameter. The target was then bombarded with 65 MeV alpha-beam from the SF cyclotron and the elastically scattered beam was detected at 11°. The yield was compared with those measured at the same condition for a thin Ni foil with known thickness. Figure 15 shows the target thickness as a function of

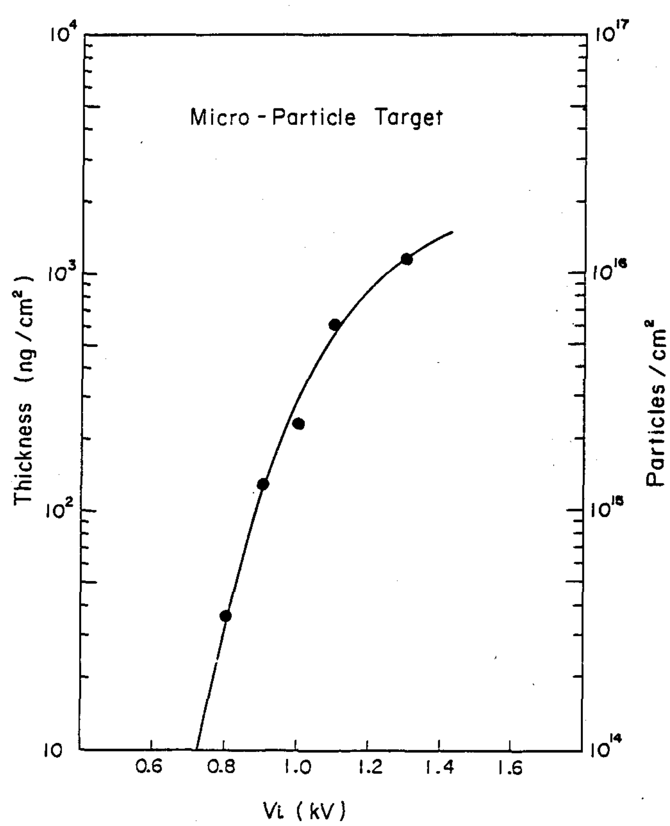

Fig. 15. Thickness of the nickel microparticle target as a function of source voltage.

the ion source voltage. The allowable range of the internal target thickness depends on the luminosity and the beam lifetime. The minimum thickness is bounded by the minimum counting rate requirements. On the other hand, the maximum is limited by the decaying time of the stored ion beam[16]. The obtained thickness between 10 and 1000 ng/cm^2 is suitable for the practical use as an internal target. The thickness is easily controllable by changing the ion-source voltage. The observed energy spectrum of the elastically scattered ions was asymmetric in shape with a tail at the low energy side. It can be compared with the curve deduced from the measured particle size which has a logarithmic-normal distribution. The ion energy in actual use for the internal target is much higher than the one in this experiment. Therefore it seems to be possible to do high resolution studies with this target at higher energies. The life time of the target is around 5 hours. So far we have tested molybdenum and tungsten microparticles as well as nickel and obtained similar results. A little loss of microparticles through the openings needed for the passage of ion beams turned out to be a problem. Once this obstacle is overcome this internal target system seems to be a promising method.

Status (August 1986) and Prospects

For the TARN II ring, we have already completed the whole magnet system and the power supply for the dipole magnets. The magnetic fields of all of the dipoles and quadrupoles have been measured in detail. The magnet system will then be installed exactly at the designated ring positions in this month. The rf cavity and the electrostatic septum for the extraction have been completed. The vacuum chamber of the ring has just been ordered. For most of the other components, the existing devices of the old TARN will be used again. We intend to start the first beam test during 1987.

For the electron cooling system, main parts of the cooling device have already been made. The high current electron beam will be produced in 1987 and its properties will be studied in the test. The cooling of the ion beam is scheduled to start in 1988.

Acknowledgements

The author would like to thank all of the staff at INS who contributed to the design and construction of this project. Many thanks are due to members of the machine shop for their support and also members of the computer section for the use of the FACOM M-380 computer. The electron cooling project was supported by the Grant for Scientific Research of the Ministry of Education, Science and Culture.

References

1. Y. Hirao et al., IEEE Trans. NS-26 (1979) 3730.
2. A. Noda et al., IEEE Trans. NS-32 (1985) 2684.
3. K. Sato et al., IEEE Trans. NS-32 (1985) 2828.
4. Y. Hirao et al., Proc. of the 7th Int. Conf. on Cyclotrons and their Applications (Birkhäuser, Basel, 1975), p.103.
5. I. Sugai, Nucl. Instr. and Meth. A236 (1985) 576.
6. N. Ueda et al., IEEE Trans. NS-32 (1985) 3178.
7. M. Takanaka et al., IEEE Trans. NS-32 (1985) 2436.
8. T. Tanabe et al., Proc. of the Workshop on Electron Cooling and Related Applications, Karlsruhe, KfK 3846 (1984) 127.
9. T. Tanabe et al., IEEE Trans. NS-32 (1985) 2412.
10. W. B. Herrmansfeldt, SLAC Report 226 (1979).
11. T. Ellison et al., Fermilab $\bar{p}$ Note 259 (1983).
12. H. Poth et al., to be published in Nucl. Instr. and Meth.
13. T. Tanabe et al., Institute for Nuclear Study report INS-T-454 (1986).
14. T. Ellison, IEEE Trans. NS-32 (1985) 2418.
15. H. O. Meyer, Proc. of the CEBAF Workshop (1985).
16. H. O. Meyer, Nucl. Instr. and Meth. B10/11 (1985) 342.